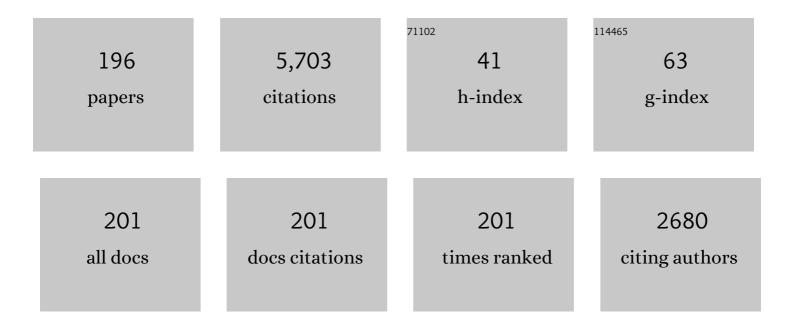
Changhee Lee

List of Publications by Year in descending order

Source: https://exaly.com/author-pdf/3245451/publications.pdf Version: 2024-02-01



#	Article	IF	CITATIONS
1	Kinetics Study on Low-Temperature Tempering of Martensitic Phase in Medium Mn Steel Weldment During Paint-Baking Heat Treatment. Metals and Materials International, 2022, 28, 1157-1168.	3.4	7
2	Nature of nonmetallic inclusions in electrogas weld metal. Welding in the World, Le Soudage Dans Le Monde, 2022, 66, 379-390.	2.5	3
3	Heat-Affected Zone Characteristics with Post-Weld Heat Treatments in Austenitic Fe–Mn–Al–C Lightweight Steels. Metals and Materials International, 2022, 28, 2371-2380.	3.4	3
4	Surface Metallization and Ceramic Deposition on Thermoplastic-Polymer and Thermosetting-Polymer Composite Via Atmospheric Plasma Spraying. Metals and Materials International, 2021, 27, 3293-3306.	3.4	3
5	Fusion Weldabilities of Advanced High Manganese Steels: A Review. Metals and Materials International, 2021, 27, 2046.	3.4	24
6	Shock Absorption Effect on Particle Fragmentation and Microstructural Features of Vacuum-Kinetic-Sprayed Al2O3 Film on Polycarbonate Substrate. Journal of Thermal Spray Technology, 2021, 30, 558-570.	3.1	1
7	Impact Behavior for Successful Particle–Particle Bonding in Vacuum Kinetic Spraying. Journal of Thermal Spray Technology, 2021, 30, 542-557.	3.1	10
8	Influence of alloying elements in low temperature transformation Weldment on Ms. temperature, microstructure and mechanical properties. Materials Characterization, 2021, 171, 110755.	4.4	2
9	Characterization of the local brittle layer formed in electro-gas weld metals. Welding in the World, Le Soudage Dans Le Monde, 2021, 65, 513-524.	2.5	3
10	Relationship between Residual Stress and Net Strain in Low-Temperature Transformation Weldments Considering Microstructure. Metals, 2021, 11, 755.	2.3	0
11	Effect of Microstructure on Low-Temperature Impact Toughness of Multi-Pass Weld Metal of 1 GPa Class High Strength Steel. Journal of Welding and Joining, 2021, 39, 233-238.	1.3	4
12	Review on the Resistance Spot Weldability of Medium-Mn TRIP steel. Journal of Welding and Joining, 2021, 39, 239-245.	1.3	2
13	Phase transformation and the mechanical characteristics of heat-affected zones in austenitic Fe–Mn–Al–Cr–C lightweight steel during post-weld heat treatment. Materials Characterization, 2021, 177, 111150.	4.4	9
14	Effect of Surface Smoothness on the Structure of Scale and Formation of Surface Cracks in TiAl Alloys under Heat Treatment. Metal Science and Heat Treatment, 2021, 63, 414.	0.6	0
15	Enhancing the deposition capability of Cr3C2–NiCr in kinetic spraying via damage accumulation in feedstock powder. Ceramics International, 2020, 46, 1104-1110.	4.8	1
16	Microstructural and Inclusion Characteristics of C–Mn Steel Welds at a Minimal Level of Titanium. Metals and Materials International, 2020, 26, 1226-1234.	3.4	11
17	Tribological and Microstructural Properties of Carbon Steel Coatings Fabricated by Wire Arc Spray. Metals and Materials International, 2020, 26, 650-659.	3.4	3
18	Promotion of the fragmentation and densification for a dense vacuum kinetic-sprayed Y2O3 coating by heat-treatment of feedstock powder. Ceramics International, 2020, 46, 9016-9024.	4.8	10

#	Article	IF	CITATIONS
19	Reactivity Enhancement and Fabrication of Al-MoO3 Thermite Coating Using Ball Milling for Kinetic Spraying. Journal of Thermal Spray Technology, 2020, 29, 1669-1681.	3.1	2
20	Bonding formation in vacuum kinetic-sprayed Y2O3 particles induced by high-velocity impact. Surface and Coatings Technology, 2020, 394, 125866.	4.8	6
21	A new class of lightweight, stainless steels with ultra-high strength and large ductility. Scientific Reports, 2020, 10, 12140.	3.3	46
22	Correlation of Plasma Erosion Resistance and the Microstructure of YF3 Coatings Prepared by Vacuum Kinetic Spray. Journal of Thermal Spray Technology, 2020, 29, 1016-1026.	3.1	2
23	Local variation of impact toughness in tandem electro-gas welded joint. Welding in the World, Le Soudage Dans Le Monde, 2020, 64, 457-465.	2.5	3
24	Effects of in-situ post-weld heat treatment on the microstructure and mechanical properties of the coarse-grained heat-affected zone in a resistance spot weld in medium Mn TRIP steel. Materials Science & amp; Engineering A: Structural Materials: Properties, Microstructure and Processing, 2020, 788, 139477.	5.6	12
25	Local brittle cracking in the heat-affected zone of lightweight steels. Materials Chemistry and Physics, 2019, 238, 121904.	4.0	9
26	Quantitative Evaluation of Nucleation Potency of Ti-containing Inclusions for Acicular Ferrite. ISIJ International, 2019, 59, 1105-1112.	1.4	9
27	Computational Research on Factors Affecting Particle Velocity in a Vacuum Kinetic Spray Process. Journal of Thermal Spray Technology, 2019, 28, 1945-1958.	3.1	18
28	Consideration of the criteria for successful deposition in cermet kinetic spraying using WC-17Co powder. Surface and Coatings Technology, 2019, 361, 314-323.	4.8	2
29	Remarkable improvement in resistance spot weldability of medium-Mn TRIP steel by paint-baking heat treatment. Materials Science & Engineering A: Structural Materials: Properties, Microstructure and Processing, 2019, 766, 138401.	5.6	29
30	Roles of (Fe, Mn)3Al Precipitates and MBIP on the Hot Ductility Behavior of Fe–30Mn–9Al–0.9C Lightweight Steels. Metals and Materials International, 2019, 25, 1019-1026.	3.4	15
31	The importance of intimate inter-crystallite bonding for the plasma erosion resistance of vacuum kinetic sprayed Y2O3 coating. Surface and Coatings Technology, 2019, 374, 493-499.	4.8	19
32	A comparison of cross-tension properties and fracture behavior between similar and dissimilar resistance spot-weldments in medium-Mn TRIP steel. Materials Science & Engineering A: Structural Materials: Properties, Microstructure and Processing, 2019, 752, 206-216.	5.6	40
33	Microstructural evolution of laser-brazed joint of Mg2Si and HMS on DBC substrate for thermoelectric generator. Materials Chemistry and Physics, 2019, 227, 352-357.	4.0	4
34	Formation of Secondary Phases and Their Effect on the Mechanical Properties of Joints Formed by TLP Bonding Using Fe–B–Si Insert Metal in Duplex Stainless Steel. Metals and Materials International, 2019, 25, 425-438.	3.4	10
35	Characterization of Mechanical and Metallurgical Notch Effects of DP980 Steel Weld Joints in Fatigue Performance. Metallurgical and Materials Transactions A: Physical Metallurgy and Materials Science, 2019, 50, 1294-1307.	2.2	10
36	Performance Comparison of Double-Layer Liner for Shaped Charge Fabricated Using Kinetic Spray. Journal of Thermal Spray Technology, 2019, 28, 484-494.	3.1	9

#	Article	IF	CITATIONS
37	Precipitation behavior and its effect on mechanical properties in weld heat-affected zone in age hardened FeMnAlC lightweight steels. Materials Science & Engineering A: Structural Materials: Properties, Microstructure and Processing, 2019, 742, 61-68.	5.6	27
38	Nucleation Behavior of Acicular Ferrite in 1 GPa Class High Strength Steel Weld Metal. Journal of Welding and Joining, 2019, 37, 21-26.	1.3	5
39	Investigations of the microstructure evolution and tensile deformation behavior of austenitic Fe-Mn-Al-C lightweight steels and the effect of Mo addition. Acta Materialia, 2018, 147, 226-235.	7.9	87
40	Influence of Si on sigma phase precipitation and pitting corrosion in superaustenitic stainless steel weld metal. Materials Chemistry and Physics, 2018, 207, 91-97.	4.0	42
41	Microstructure control to improve creep strength of alumina-forming austenitic heat-resistant steel by pre-strain. Materials Characterization, 2018, 137, 1-8.	4.4	33
42	Influence of κ-carbide precipitation on the microstructure and mechanical properties in the weld heat-affected zone in various FeMnAlC alloys. Materials Science & Engineering A: Structural Materials: Properties, Microstructure and Processing, 2018, 726, 223-230.	5.6	24
43	Characteristics of kinetic sprayed Ta in terms of the deposition behavior, microstructural evolution and mechanical properties: Effect of strain-rate-dependent response of Ta at high temperature. Materials Characterization, 2018, 141, 49-58.	4.4	9
44	Improvement of circumferential ductility by reducing discontinuities in a high-Mn TWIP steel weldment. Materials Characterization, 2018, 139, 293-302.	4.4	11
45	Correlation Between Microstructure and Low-Temperature Impact Toughness of Simulated Reheated Zones in the Multi-pass Weld Metal of High-Strength Steel. Metallurgical and Materials Transactions A: Physical Metallurgy and Materials Science, 2018, 49, 177-186.	2.2	18
46	Roles of Particle Size Distribution in Bimodal Feedstocks on the Deposition Behavior and Film Properties in Vacuum Kinetic Spraying. Journal of Thermal Spray Technology, 2018, 27, 857-869.	3.1	10
47	Possibility of Mn substitution of Ni through evaluation of mechanical properties and corrosion resistance in superaustenitic stainless steel weld metal. Materials Science & Engineering A: Structural Materials: Properties, Microstructure and Processing, 2018, 733, 16-23.	5.6	16
48	Precipitation behavior of the sigma phase with Ni and Mn content variations in superaustenitic stainless steel weld metal. Materials Characterization, 2018, 144, 148-154.	4.4	29
49	Improved creep strength of alumina-forming austenitic heat-resistant steels through W addition. Materials Science & Engineering A: Structural Materials: Properties, Microstructure and Processing, 2017, 696, 70-79.	5.6	28
50	Hot deformation behavior and microstructural evolution of alumina-forming austenitic heat-resistant steels during hot compression. Materials Characterization, 2017, 123, 207-217.	4.4	27
51	The role of phosphorus in precipitation behavior and its effect on the creep properties of alumina-forming austenitic heat-resistant steels. Materials Science & Engineering A: Structural Materials: Properties, Microstructure and Processing, 2017, 684, 14-21.	5.6	13
52	Inflight Particle Behavior in the Vacuum Kinetic Spray Process. Journal of Thermal Spray Technology, 2017, 26, 1616-1631.	3.1	21
53	Microstructure Evolution and Age-Hardening Behavior of Microalloyed Austenitic Fe-30Mn-9Al-0.9C Light-Weight Steels. Metallurgical and Materials Transactions A: Physical Metallurgy and Materials Science, 2017, 48, 4500-4510.	2.2	43
54	Correlation of Fracture Mode Transition of Ceramic Particle with Critical Velocity for Successful Deposition in Vacuum Kinetic Spraying Process. Journal of Thermal Spray Technology, 2017, 26, 327-339.	3.1	25

#	Article	IF	CITATIONS
55	Microstructural features affecting optical properties of vacuum kinetic sprayed Al2O3 thin film. Surfaces and Interfaces, 2017, 9, 114-123.	3.0	10
56	Microstructure and Mechanical Properties of Reheated Zones in the Multi-pass Weld Metal of High-Strength Steel. Journal of Welding and Joining, 2017, 35, 21-26.	1.3	5
57	Kinetic Spraying Deposition of Reactive-Enhanced Al-Ni Composite for Shaped Charge Liner Applications. Journal of Thermal Spray Technology, 2016, 25, 483-493.	3.1	11
58	Factors Affecting the Inclusion Potency for Acicular Ferrite Nucleation in High-Strength Steel Welds. Metallurgical and Materials Transactions A: Physical Metallurgy and Materials Science, 2016, 47, 2842-2854.	2.2	64
59	Correlation of microstructure with tribological properties in atmospheric plasma sprayed Mo-added ferrous coating. Surface and Coatings Technology, 2016, 307, 908-914.	4.8	11
60	Influence of substrate roughness on bonding mechanism in cold spray. Surface and Coatings Technology, 2016, 304, 592-605.	4.8	62
61	Hot ductility and hot cracking susceptibility of Ti-modified austenitic high Mn steel weld HAZ. Materials Chemistry and Physics, 2016, 184, 118-129.	4.0	7
62	Correlation of Impact Conditions, Interface Reactions, Microstructural Evolution, and Mechanical Properties in Kinetic Spraying of Metals: A Review. Journal of Thermal Spray Technology, 2016, 25, 1461-1489.	3.1	11
63	Characterization of bond line discontinuities in a high-Mn TWIP steel pipe welded by HF-ERW. Materials Characterization, 2016, 118, 14-21.	4.4	13
64	Effect of thermal and thermo-mechanical cycling on the boron segregation behavior in the coarse-grained heat-affected zone of low-alloy steel. Materials Characterization, 2016, 116, 65-75.	4.4	14
65	Effect of intermetallic compounds on the bonding state of kinetic sprayed Al deposit on Cu after heat-treatment. Surface and Coatings Technology, 2016, 302, 39-46.	4.8	6
66	Formation and heat treatment of kinetic sprayed nanocrystalline Al coatings reinforced with multi-walled carbon nanotubes: The relationship between microstructural features and physical properties. Surface and Coatings Technology, 2016, 289, 124-135.	4.8	7
67	Characterization of Inclusions Formed in Ti-containing Steel Weld Metals. ISIJ International, 2015, 55, 1730-1738.	1.4	20
68	Influence of Cr on Weld Solidification Cracking in Fe-15Mn-0.5C-3.5Al-xCr Alloys. ISIJ International, 2015, 55, 257-263.	1.4	5
69	Variation in the Chemical Driving Force for Intragranular Nucleation in the Multi-pass Weld Metal of Ti-Containing High-Strength Low-Alloy Steel. Metallurgical and Materials Transactions A: Physical Metallurgy and Materials Science, 2015, 46, 3581-3591.	2.2	20
70	Role of spray processes on microstructural evolution, and physical and mechanical properties of multi-walled carbon nanotube reinforced cu composite coatings. Applied Surface Science, 2015, 356, 1039-1051.	6.1	18
71	Shock-induced plasticity and fragmentation phenomena during alumina deposition in the vacuum kinetic spraying process. Scripta Materialia, 2015, 100, 44-47.	5.2	40
72	Dynamic fragmentation process and fragment microstructure evolution of alumina particles in a vacuum kinetic spraying system. Scripta Materialia, 2015, 108, 72-75.	5.2	25

#	Article	IF	CITATIONS
73	Deposition of Workability-Enhancing Disposable Thick Fe Deposits on Fe-Si Alloy Sheets Using Thermal and Kinetic Spray Processes. Journal of Thermal Spray Technology, 2015, 24, 318-327.	3.1	0
74	Microstructure of Kinetic Spray Coatings: A Review. Journal of Thermal Spray Technology, 2015, 24, 592-610.	3.1	103
75	Formation of Mn-depleted zone in Ti-containing weld metals. Welding in the World, Le Soudage Dans Le Monde, 2015, 59, 373-380.	2.5	29
76	Residual stress and crack initiation in laser clad composite layer with Co-based alloy and WC + NiCr. Applied Surface Science, 2015, 345, 286-294.	6.1	96
77	Effect of tungsten addition on high-temperature properties and microstructure of alumina-forming austenitic heat-resistant steels. Materials Science & Engineering A: Structural Materials: Properties, Microstructure and Processing, 2015, 647, 163-169.	5.6	34
78	Microstructural evolution and solidification cracking susceptibility of Fe–18Mn–0.6C–xAl steel welds. Journal of Materials Science, 2015, 50, 279-286.	3.7	41
79	Room Temperature Synthesis of Highly Compact TiO2 Coatings by Vacuum Kinetic Spraying to Serve as a Blocking Layer in Polymer Electrolyte-Based Dye-Sensitized Solar Cells. Journal of Thermal Spray Technology, 2015, 24, 328-337.	3.1	10
80	Investigating the Cause of Hindrance to the Interfacial Bonding of INCONEL 718 Layer Deposited by Kinetic Spray Process. Journal of the Korean Institute of Surface Engineering, 2015, 48, 275-282.	0.1	2
81	Effect of Restraint Stress on the Precipitation Behavior and Thermal Fatigue Properties of Simulated Weld Heat Affected Zone in Ferritic Stainless Steel. Journal of Welding and Joining, 2015, 33, 6-12.	1.3	1
82	Effect of silicon on the solidification cracking behavior and metastable carbide formation in austenitic high Mn steel welds. Materials Chemistry and Physics, 2014, 148, 499-502.	4.0	8
83	Influence of Ti on non-metallic inclusion formation and acicular ferrite nucleation in high-strength low-alloy steel weld metals. Metals and Materials International, 2014, 20, 119-127.	3.4	63
84	Effect of gas flow rate on deposition behavior of Fe-based amorphous alloys in vacuum kinetic spray process. Surface and Coatings Technology, 2014, 259, 585-593.	4.8	35
85	Effect of Ni on the hot ductility and hot cracking susceptibility of high Mn austenitic cast steel. Materials Science & Engineering A: Structural Materials: Properties, Microstructure and Processing, 2014, 618, 295-304.	5.6	31
86	Mn-Depleted Zone Formation in Rapidly Cooled High-Strength Low-Alloy Steel Welds. Metallurgical and Materials Transactions A: Physical Metallurgy and Materials Science, 2014, 45, 4753-4757.	2.2	23
87	Oxide Formation Mechanisms in High Manganese Steel Welds. Metallurgical and Materials Transactions A: Physical Metallurgy and Materials Science, 2014, 45, 2046-2054.	2.2	25
88	Bonding, Reactivity, and Mechanical Properties of the Kinetic-Sprayed Deposition of Al for a Thermally Activated Reactive Cu Liner. Journal of Thermal Spray Technology, 2014, 23, 818-826.	3.1	19
89	Effect of titanium content on weld microstructure and mechanical properties of bainitic GMA welds. Welding in the World, Le Soudage Dans Le Monde, 2014, 58, 893-901.	2.5	14
90	Correlation between microstructure and mechanical properties of heat affected zones in Fe–8Mn–0.06C steel welds. Materials Chemistry and Physics, 2014, 146, 175-182.	4.0	16

#	Article	IF	CITATIONS
91	Research on Acceleration Mechanism of Inflight Particle and Gas Flow Effect for the Velocity Control in Vacuum Kinetic Spray Process. Korean Journal of Materials Research, 2014, 24, 98-104.	0.2	1
92	Property Evaluation of Kinetic Sprayed Al-Ni Composite Coatings. Journal of Welding and Joining, 2014, 32, 72-79.	1.3	1
93	Deposition Behavior and Microstructural Features of Vacuum Kinetic Sprayed Aluminum Nitride. Journal of Thermal Spray Technology, 2013, 22, 882-891.	3.1	12
94	Restoration of face-centered cubic metals subjected to kinetic spraying. Metals and Materials International, 2013, 19, 283-293.	3.4	0
95	Characteristics of inclusions in rutile-type FCAW weld metal. Welding in the World, Le Soudage Dans Le Monde, 2013, 57, 65-72.	2.5	11
96	Effect of Process Gas Flow on the Coating Microstructure and Mechanical Properties of Vacuum Kinetic-Sprayed TiN Layers. Journal of Thermal Spray Technology, 2013, 22, 1109-1119.	3.1	26
97	Effect of Plasma Nitriding and Nitrocarburizing on HVOF-Sprayed Stainless Steel Coatings. Journal of Thermal Spray Technology, 2013, 22, 1366-1373.	3.1	17
98	Different aspect of pitting corrosion and interphase corrosion in the weld heat-affected zone of high-nitrogen Fe–18Cr–10Mn–N steel. Materials Chemistry and Physics, 2013, 142, 556-563.	4.0	21
99	Role of Ca treatment in hydrogen induced cracking of hot rolled API pipeline steel in acid sour media. Metals and Materials International, 2013, 19, 45-48.	3.4	57
100	Microstructure Evolution of Titanium Nitride Film during Vacuum Kinetic Spraying. Journal of the American Ceramic Society, 2013, 96, 40-43.	3.8	66
101	Variation in microstructures and mechanical properties in the coarse-grained heat-affected zone of low-alloy steel with boron content. Materials Science & Engineering A: Structural Materials: Properties, Microstructure and Processing, 2013, 559, 178-186.	5.6	31
102	Corrosion fatigue behaviors of HSB800 and its HAZs in air and seawater environments. Materials Science & Engineering A: Structural Materials: Properties, Microstructure and Processing, 2013, 559, 751-758.	5.6	12
103	Amorphization of ZrO2Â+ÂCeO2 Powders Through Mechanical Milling for the Use of Kinetic Spray. Journal of Materials Engineering and Performance, 2013, 22, 3717-3722.	2.5	3
104	Manufacturing and Compressive Deformation Behavior of High-Strength Aluminum Coating Material Fabricated by Kinetic Spray Process. Metallurgical and Materials Transactions A: Physical Metallurgy and Materials Science, 2013, 44, 4876-4879.	2.2	7
105	Effect of Ti Addition on Weld Microstructure and Inclusion Characteristics of Bainitic GMA Welds. ISIJ International, 2013, 53, 880-886.	1.4	31
106	Influence of Oxygen Content on Microstructure and Inclusion Characteristics of Bainitic Weld Metals. ISIJ International, 2013, 53, 279-285.	1.4	18
107	Microstructure Evolution and Its Effect on Strength during Thermo-mechanical Cycling in the Weld Coarse-grained Heat-affected Zone of Ti-Nb Added HSLA Steel. Journal of Welding and Joining, 2013, 31, 44-49.	0.3	5
108	Strengthening mechanisms of multiwalled carbon nanotube-reinforced Cu nanocomposite coatings during kinetic spray consolidation. Journal of Materials Research, 2012, 27, 2375-2381.	2.6	3

#	Article	IF	CITATIONS
109	Mechanical property enhancement of kinetic sprayed Al coatings reinforced by multi-walled carbon nanotubes. Acta Materialia, 2012, 60, 5031-5039.	7.9	29
110	Nanoscale deformation twinning at ultrahigh strain rates during kinetic spraying of nickel. Materials Letters, 2012, 89, 320-323.	2.6	14
111	Effects of alloying elements on the thermal fatigue properties of the 15wt% Cr ferritic stainless steel weld HAZ. Materials Science & Engineering A: Structural Materials: Properties, Microstructure and Processing, 2012, 555, 44-51.	5.6	10
112	Effect of Complex Inclusion Particles on the Solidification Structure of Fe-Ni-Mn-Mo Alloy. Metallurgical and Materials Transactions B: Process Metallurgy and Materials Processing Science, 2012, 43, 1550-1564.	2.1	75
113	Behavior of Cu precipitates during thermo-mechanical cycling in the weld CGHAZ of Cu-containing HSLA steel. Metals and Materials International, 2012, 18, 857-862.	3.4	6
114	Cold cracking susceptibility of boron added high-strength bainitic steels. Metals and Materials International, 2012, 18, 1029-1036.	3.4	6
115	Liquation behavior in the weld HAZ of high Si nodular iron. Metals and Materials International, 2012, 18, 371-377.	3.4	0
116	Correlation of particle impact conditions with bonding, nanocrystal formation and mechanical properties in kinetic sprayed nickel. Acta Materialia, 2012, 60, 3524-3535.	7.9	80
117	Thermally activated reactions of multi-walled carbon nanotubes reinforced aluminum matrix composite during the thermal spray consolidation. Materials Chemistry and Physics, 2012, 133, 495-499.	4.0	31
118	Effects of post-weld heat treatment cycles on microstructure and mechanical properties of electric resistance welded pipe welds. Materials & Design, 2012, 34, 685-690.	5.1	24
119	The effect of the precipitates type on the thermal fatigue properties of 18% Cr ferritic stainless steel weld HAZ. Materials Science & Engineering A: Structural Materials: Properties, Microstructure and Processing, 2012, 546, 97-102.	5.6	13
120	Electrical and mechanical properties of multi-walled carbon nanotube reinforced Al composite coatings fabricated by high velocity oxygen fuel spraying. Surface and Coatings Technology, 2012, 206, 4060-4067.	4.8	10
121	Microstructure and texture of Al coating during kinetic spraying and heat treatment. Journal of Materials Science, 2012, 47, 4053-4061.	3.7	34
122	Interfacial bonding and microstructural evolution of Al in kinetic spraying. Journal of Materials Science, 2012, 47, 4649-4659.	3.7	32
123	Grain Size of Acicular Ferrite in Ferritic Weld Metal. Welding in the World, Le Soudage Dans Le Monde, 2011, 55, 36-40.	2.5	3
124	Formation of coating and tribological behavior of kinetic sprayed Fe-based bulk metallic glass. Journal of Alloys and Compounds, 2011, 509, 347-353.	5.5	56
125	Fatigue crack growth behavior of the simulated HAZ of 800MPa grade high-performance steel. Materials Science & Engineering A: Structural Materials: Properties, Microstructure and Processing, 2011, 528, 2331-2338.	5.6	62
126	Enhancement of metallic glass properties of Cu-based BMG coating by shroud plasma spraying. Surface and Coatings Technology, 2011, 205, 3020-3026.	4.8	21

#	Article	IF	CITATIONS
127	Variation of microstructures and mechanical properties in the post-weld heat-treated HAZ of Cu containing HSLA steel welds. Metals and Materials International, 2011, 17, 137-142.	3.4	8
128	Influence of the interface temperature and strain gradients on the impact energy model of a soft particle on a hard substrate during kinetic spraying. Metals and Materials International, 2011, 17, 335-340.	3.4	7
129	Evaluation of Die-Soldering and Erosion Resistance of High Velocity Oxy-Fuel Sprayed MoB-Based Cermet Coatings. Journal of Thermal Spray Technology, 2011, 20, 1022-1034.	3.1	14
130	Dependence of Bonding Mechanisms of Cold Sprayed Coatings on Strain-Rate-Induced Non-Equilibrium Phase Transformation. Journal of Thermal Spray Technology, 2011, 20, 860-865.	3.1	41
131	Effect of thermo-mechanical cycling on the microstructure and strength of lath martensite in the weld CGHAZ of HSLA steel. Materials Science & Engineering A: Structural Materials: Properties, Microstructure and Processing, 2011, 528, 7658-7662.	5.6	36
132	Effects of alloying elements on the thermal fatigue properties of the ferritic stainless steel weld HAZ. Procedia Engineering, 2011, 10, 383-389.	1.2	12
133	Cracking behavior in a dissimilar weld between high silicon nodular cast iron and ferritic stainless steel. Metals and Materials International, 2010, 16, 483-488.	3.4	10
134	An Experimental and Finite Element Study of Cold Spray Copper Impact onto Two Aluminum Substrates. Journal of Thermal Spray Technology, 2010, 19, 620-634.	3.1	159
135	The Effects of Successive Impacts and Cold Welds on the Deposition Onset of Cold Spray Coatings. Journal of Thermal Spray Technology, 2010, 19, 575-585.	3.1	60
136	Effect of Thermally Softened Bronze Matrix on the Fracturing Behavior of Diamond Particles in Hybrid Sprayed Bronze/Diamond Composite. Journal of Thermal Spray Technology, 2010, 19, 902-910.	3.1	1
137	Nanostructure formation and its effects on the mechanical properties of kinetic sprayed titanium coating. Materials Science & Engineering A: Structural Materials: Properties, Microstructure and Processing, 2010, 527, 6313-6319.	5.6	54
138	Effect of particle size on the microstructure and properties of kinetic sprayed nickel coatings. Surface and Coatings Technology, 2010, 204, 3326-3335.	4.8	50
139	Tribological behavior of B4C reinforced Fe-base bulk metallic glass composite coating. Surface and Coatings Technology, 2010, 205, 1962-1968.	4.8	59
140	Oxidation and crystallization mechanisms in plasma-sprayed Cu-based bulk metallic glass coatings. Acta Materialia, 2010, 58, 952-962.	7.9	43
141	Effect of powder state on the deposition behaviour and coating development in kinetic spray process. Journal Physics D: Applied Physics, 2009, 42, 075305.	2.8	11
142	Dependence of initial powder temperature on impact behaviour of bulk metallic glass in a kinetic spray process. Journal Physics D: Applied Physics, 2009, 42, 082004.	2.8	12
143	Deposition characteristics of copper particles on roughened substrates through kinetic spraying. Applied Surface Science, 2009, 255, 3472-3479.	6.1	51
144	Characteristics and heat treatment of cold-sprayed Al–Sn binary alloy coatings. Applied Surface Science, 2009, 255, 3933-3939.	6.1	49

#	Article	IF	CITATIONS
145	Development of cermet coatings by kinetic spray technology for the application of die-soldering and erosion resistance. Surface and Coatings Technology, 2009, 204, 345-352.	4.8	21
146	Advanced deposition characteristics of kinetic sprayed bronze/diamond composite by tailoring feedstock properties. Composites Science and Technology, 2009, 69, 463-468.	7.8	41
147	Behavior of (Ti, Nb)(C, N) complex particle during thermomechanical cycling in the weld CGHAZ of a microalloyed steel. Acta Materialia, 2009, 57, 2311-2320.	7.9	42
148	Bonding features and associated mechanisms in kinetic sprayed titanium coatings. Acta Materialia, 2009, 57, 5654-5666.	7.9	262
149	Strain-enhanced nanocrystallization of a CuNiTiZr bulk metallic glass coating by a kinetic spraying process. Acta Materialia, 2009, 57, 6191-6199.	7.9	52
150	Phase dependence of Fe-based bulk metallic glasses on properties of thermal spray coatings. Journal of Alloys and Compounds, 2009, 475, L9-L12.	5.5	31
151	Phase separation in kinetic sprayed bulk metallic glasses. Journal Physics D: Applied Physics, 2009, 42, 182007.	2.8	6
152	Effects of Silver Addition on Properties and Performance of Plasma Sprayed La0.6Sr0.4Co0.2Fe0.8O3â~δ Interconnect Layer. Journal of Thermal Spray Technology, 2008, 17, 708-714.	3.1	11
153	Effect of vitreous enamel coating on the oxidation behavior of Ti6Al4V and TiAl alloys at high temperatures. Journal of Coatings Technology Research, 2008, 5, 93-98.	2.5	22
154	Orowan strengthening effect on the nanoindentation hardness of the ferrite matrix in microalloyed steels. Materials Science & Engineering A: Structural Materials: Properties, Microstructure and Processing, 2008, 487, 552-557.	5.6	102
155	Effect of Cu and B addition on tempering behavior in the weld CGHAZ of high strength low alloy plate steel. Materials Science & Engineering A: Structural Materials: Properties, Microstructure and Processing, 2008, 497, 153-159.	5.6	10
156	The influence of process parameters on deposition characteristics of a soft/hard composite coating in kinetic spray process. Applied Surface Science, 2008, 254, 2269-2275.	6.1	32
157	General aspects of interface bonding in kinetic sprayed coatings. Acta Materialia, 2008, 56, 4858-4868.	7.9	379
158	Development and microstructure optimization of atmospheric plasma-sprayed NiO/YSZ anode coatings for SOFCs. Surface and Coatings Technology, 2008, 202, 3180-3186.	4.8	21
159	Particle coarsening kinetics considering critical particle size in the presence of multiple particles in the heat-affected zone of a weld. Materials Science & Engineering A: Structural Materials: Properties, Microstructure and Processing, 2008, 483-484, 633-636.	5.6	9
160	Oxidation dependency of critical velocity for aluminum feedstock deposition in kinetic spraying process. Materials Science & Engineering A: Structural Materials: Properties, Microstructure and Processing, 2008, 486, 300-307.	5.6	85
161	Tribological behavior of NiCr-base blended and nanostructured composite APS coatings by rig test. Wear, 2008, 265, 1565-1571.	3.1	9
162	Oxidation behavior of bulk amorphous Ni57Ti18Zr20Si3Sn2 coatings between 473 and 973K in air. Journal of Alloys and Compounds, 2008, 449, 384-388.	5.5	6

#	Article	IF	CITATIONS
163	Dynamic amorphization and recrystallization of metals in kinetic spray process. Applied Physics Letters, 2008, 92, .	3.3	78
164	The Fabrication of Carbon Nanotubes Reinforced Copper Coating by a Kinetic Spray Process. Journal of Nanoscience and Nanotechnology, 2008, 8, 5561-5565.	0.9	8
165	Tribological behavior of the kinetic sprayed Ni59Ti16Zr20Si2Sn3 bulk metallic glass. Journal of Alloys and Compounds, 2007, 434-435, 64-67.	5.5	14
166	Fabrication of automotive heat exchanger using kinetic spraying process. Surface and Coatings Technology, 2007, 201, 9524-9532.	4.8	18
167	Impacting behavior of bulk metallic glass powder at an abnormally high strain rate during kinetic spraying. Materials Science & Engineering A: Structural Materials: Properties, Microstructure and Processing, 2007, 449-451, 911-915.	5.6	29
168	Evaluation of the effects of the crystallinity of kinetically sprayed Ni–Ti–Zr–Si–Sn bulk metallic glass on the scratch response. Materials Science & Engineering A: Structural Materials: Properties, Microstructure and Processing, 2007, 449-451, 285-289.	5.6	27
169	Influence of Nb addition on the particle coarsening and microstructure evolution in a Ti-containing steel weld HAZ. Materials Science & Engineering A: Structural Materials: Properties, Microstructure and Processing, 2007, 454-455, 648-653.	5.6	24
170	Prediction for the austenite grain size in the presence of growing particles in the weld HAZ of Ti-microalloyed steel. Materials Science & Engineering A: Structural Materials: Properties, Microstructure and Processing, 2007, 459, 40-46.	5.6	88
171	Comparison of solid oxide fuel cell anode coatings prepared from different feedstock powders by atmospheric plasma spray method. Journal of Power Sources, 2007, 171, 441-447.	7.8	19
172	Limiting austenite grain size of TiN-containing steel considering the critical particle size. Scripta Materialia, 2007, 56, 1083-1086.	5.2	26
173	Coarsening Behavior of the (Ti, Nb)(C, N) Complex Particle in a Microalloyed Steel Weld Heat-Affected Zone Considering the Critical Particle Size. Metallurgical and Materials Transactions A: Physical Metallurgy and Materials Science, 2007, 38, 2788-2795.	2.2	9
174	Effect of gas temperature on critical velocity and deposition characteristics in kinetic spraying. Applied Surface Science, 2007, 253, 3512-3520.	6.1	47
175	Critical Velocities for High Speed Particle Deposition in Kinetic Spraying. Materials Transactions, 2006, 47, 1723-1727.	1.2	23
176	Coarsening kinetics of TiN particle in a low alloyed steel in weld HAZ: Considering critical particle size. Acta Materialia, 2006, 54, 1053-1061.	7.9	56
177	The bond strength of Al–Si coating on mild steel by kinetic spraying deposition. Applied Surface Science, 2006, 252, 7809-7814.	6.1	66
178	Kinetic spraying deposition behavior of bulk amorphous NiTiZrSiSn feedstock. Materials Science & Engineering A: Structural Materials: Properties, Microstructure and Processing, 2006, 415, 45-52.	5.6	36
179	High speed impact behaviors of Al alloy particle onto mild steel substrate during kinetic deposition. Materials Science & Engineering A: Structural Materials: Properties, Microstructure and Processing, 2006, 417, 114-119.	5.6	29
180	Deposition behavior of bulk amorphous NiTiZrSiSn according to the kinetic and thermal energy levels in the kinetic spraying process. Surface and Coatings Technology, 2006, 200, 6022-6029.	4.8	62

#	Article	IF	CITATIONS
181	Effect of particle parameters on the deposition characteristics of a hard/soft-particles composite in kinetic spraying. Surface and Coatings Technology, 2006, 201, 3457-3461.	4.8	35
182	The rebound phenomenon in kinetic spraying deposition. Scripta Materialia, 2006, 54, 665-669.	5.2	126
183	Characterization of the Gas Tungsten Arc Welded Cu ₅₄ Ni ₆ Zr ₂₂ Ti ₁₈ Bulk Metallic Glass Weld. Materials Transactions, 2005, 46, 1440-1442.	1.2	16
184	Characterization of the spraying beads deposited by the kinetic spraying process. Surface and Coatings Technology, 2005, 192, 374-381.	4.8	18
185	Characterization of atmospheric plasma spray NiCr–Cr2O3–Ag–CaF2/BaF2 coatings. Surface and Coatings Technology, 2005, 195, 107-115.	4.8	35
186	Measurement of particle velocity and characterization of deposition in aluminum alloy kinetic spraying process. Applied Surface Science, 2005, 252, 1368-1377.	6.1	94
187	Phase evolutions of bulk amorphous NiTiZrSiSn feedstock during thermal and kinetic spraying processes. Scripta Materialia, 2005, 53, 125-130.	5.2	58
188	Critical factors affecting the amorphous phase formation of NiTiZrSiSn bulk amorphous feedstock in vacuum plasma spray. Journal of Materials Science, 2005, 40, 3873-3875.	3.7	10
189	Effect of in-flight particle oxidation on the phase evolution of HVOF NiTiZrSiSn bulk amorphous coating. Journal of Materials Science, 2005, 40, 6121-6126.	3.7	27
190	Effects of Inclusions and Microstructures on Impact Energy of High Heat-Input Submerged-Arc-Weld Metals. Journal of Engineering Materials and Technology, Transactions of the ASME, 2005, 127, 204-213.	1.4	25
191	Prediction Model for the Austenite Grain Size in the Coarse Grained Heat Affected Zone of Fe-C-Mn Steels: Considering the Effect of Initial Grain Size on Isothermal Growth Behavior. ISIJ International, 2004, 44, 1230-1237.	1.4	85
192	Photocatalytic properties of nano-structured TiO2 plasma sprayed coating. Surface and Coatings Technology, 2003, 173, 192-200.	4.8	110
193	Effect of dilution on the behavior of solidification cracking in PTAW overlay deposit on Ni-Base superalloys. Metals and Materials International, 2002, 8, 469-477.	3.4	25
194	Phase evolutions of plasma sprayed ceria and yttria stabilized zirconia thermal barrier coating. Journal of Materials Science Letters, 2002, 21, 1359-1361.	0.5	13
195	Cooling rate effect on phase transformation of plasma sprayed partially stabilized zirconia. Journal of Materials Science Letters, 2001, 20, 1611-1613.	0.5	12
196	Correlation Between Constituent Phase and Weld Metal Properties in Ni-Reduced Duplex Stainless Steel. Metals and Materials International, 0, , 1.	3.4	1